

Mechanism for stickiness suppression during extreme events in Hamiltonian systems

Taline Suellen Krüger,¹ Paulo Paneque Galuzio,¹ Thiago de Lima Prado,¹ Ricardo Luiz Viana,¹
 José Danilo Szezech Jr.,² and Sergio Roberto Lopes^{1,*}

¹*Departamento de Física, Universidade Federal do Paraná, 81531-980 Curitiba, PR, Brazil*

²*Departamento de Matemática e Estatística, Univ. Est. de Ponta Grossa, 84030-900, Ponta Grossa, Paraná, Brazil*

(Received 9 January 2015; revised manuscript received 19 March 2015; published 3 June 2015)

In this paper we study how hyperbolic and nonhyperbolic regions in the neighborhood of a resonant island perform an important role allowing or forbidding stickiness phenomenon around islands in conservative systems. The vicinity of the island is composed of nonhyperbolic areas that almost prevent the trajectory to visit the island edge. For some specific parameters tiny channels are embedded in the nonhyperbolic area that are associated to hyperbolic fixed points localized in the neighborhood of the islands. Such channels allow the trajectory to be injected in the inner portion of the vicinity. When the trajectory crosses the barrier imposed by the nonhyperbolic regions, it spends a long time abandoning the vicinity of the island, since the barrier also prevents the trajectory from escaping from the neighborhood of the island. In this scenario the nonhyperbolic structures are responsible for the stickiness phenomena and, more than that, the strength of the sticky effect. We show that those properties of the phase space allow us to manipulate the existence of extreme events (and the transport associated to it) responsible for the nonequilibrium fluctuation of the system. In fact we demonstrate that by monitoring very small portions of the phase space (namely, $\approx 1 \times 10^{-5}\%$ of it) it is possible to generate a completely diffusive system eliminating long-time recurrences that result from the stickiness phenomenon.

DOI: [10.1103/PhysRevE.91.062903](https://doi.org/10.1103/PhysRevE.91.062903)

PACS number(s): 05.45.Pq, 05.45.Ac, 05.60.Cd

I. INTRODUCTION

Understanding the transport properties of Hamiltonian systems is one of the major objectives in the statistical analysis of dynamical systems [1,2]. Recent works have shown that for a large class of systems, including those exhibiting mixed phase space, the transport cannot be treated considering just ergodic theory or the random phase approximation [3]. One class of such systems is low-dimensional (3/2 or 2 degrees of freedom) Hamiltonian systems (1/2 degree of freedom corresponds to a periodical disturbance). Low-dimensional Hamiltonian systems commonly exhibit nonuniform phase spaces composed of regular (islands) and chaotic regions. The interface between these regions is far from being a smooth surface, and the dynamics near the edge between chaotic and regular regions is very complex and has been not well understood so far. The complexity comes mainly due to the presence of stickiness of the boundaries of islands [4]. The sticky effect forces a trajectory injected into the boundary area to stay near the boundary for long periods of time. One of the main consequences of this phenomenon is the existence of power law tails in the Poincaré recurrence times, making the system exhibit distribution of recurrence times with algebraic decay for long times rather than an exponential decay as expected for a normal transport system [3,5–10].

Some features of the kinetics of Hamiltonian systems are important to understand anomalous transport and super diffusion. The phase space topology of these systems plays a crucial role in the anomalous transport and in sticky phenomena [11,12]. Many problems of science such as particle advection in fluids [13,14], transport in plasma fusion devices

[2,15], celestial mechanics [16], and many others have found applications in stickiness occurrences.

Previous works have studied properties of the boundaries between regular and chaotic regions focusing mainly on the role of the stickiness of the dynamics [17,18] and the cantori structures derived from the breakup of tori [19]. When the system exhibits stickiness, the dynamics of orbits in chaotic sea is observed to be intermittent, where after periods of chaotic motion away from the influence of a sticky island, the system exhibits periods of almost regular motion. However, as far as we know, no completely satisfactory theoretical explanation is available for stickiness.

In this paper we study how characteristics of the topology of the system, namely, hyperbolic and nonhyperbolic regions in the neighborhood of a resonant island, perform an important role in order to *establish the presence and, more than that, the strength of the sticky effect*. We show that the sticky effect is associated with the presence of injection channels related to the crossing of stable and unstable manifolds of hyperbolic fixed points in the vicinity of the island, allowing the trajectories to shift between sticky and nonsticky areas of the phase space. We show that the effectiveness of such channels to capture trajectories to the sticky area is closely related to the degree of hyperbolicity of the close surrounding area of hyperbolic fixed points located in the neighborhood of an island. Finally we make use of the presence of the hyperbolic channels to avoid (control) extreme recurrence events and the anomalous transport associated to it, resulting from a trajectory injection into the sticky area.

This work is organized as follows: in Sec. II we focus our attention on the model and present definitions for nonhyperbolicity of the phase space. In Sec. III we develop our main results concerning the effect of the (non)hyperbolic surrounding of resonance island in the dynamics of the system, and our conclusions are presented in Sec. IV.

*lopes@fisica.ufpr.br

II. THE MODEL

Here we characterize a hyperbolic region of the phase space \mathcal{S} as an ensemble for which the tangent phase space splits continuously into stable (SM) and an unstable (UM) manifolds. SM and UM are invariant under the system dynamics: infinitesimal displacements in the stable (unstable) direction suffer exponential decay as time goes forward (backward) [20]. In addition, it is required that the angles between the stable and unstable directions be uniformly bounded away from zero. In this way, in order to quantify the degree of nonhyperbolicity related to the phenomena we describe in this paper, let us consider an initial condition (p_0, x_0) and an unit vector \mathbf{v} , whose temporal evolution is given by

$$\mathbf{v}_{n+1} = \mathcal{J}(p_n, x_n)\mathbf{v}_n / \|\mathcal{J}(p_n, x_n)\mathbf{v}_n\|, \quad (1)$$

where $\mathcal{J}(p_n, x_n)$ is the Jacobian matrix of the map. For n large enough, \mathbf{v} is parallel to the Lyapunov vector $\mathbf{u}(p, x)$ associated to the maximum Lyapunov exponent λ_u of the map orbit starting by (p_0, x_0) . A backward iteration of the same orbit gives us a new vector \mathbf{v}_n that is parallel to the direction $\mathbf{s}(p, x)$, the Lyapunov vector associated to the minimum Lyapunov exponent λ_s [21]. For regions where $\lambda_s < 0 < \lambda_u$ the vectors $\mathbf{u}(p, x)$ and $\mathbf{s}(p, x)$ are tangent to the UM and SM, respectively, of a point (p, x) .

The (non)hyperbolic degree of a region \mathcal{S} can be studied computing the local angles between the two manifolds

$$\theta(p, x) = \cos^{-1}(|\mathbf{u} \cdot \mathbf{s}|) \quad (2)$$

for $(p, x) \in \mathcal{S}$ [22]. So $\theta(p, x) \sim 0$ denotes tangency between UM and SM at (p, x) . The general method used to calculate the θ angles follows Ref. [23].

Chaotic orbits of two-dimensional mappings are often nonhyperbolic since the SM and UM are tangent in infinitely many points. As an illustration of this effect we consider a periodically kicked rotor subjected to a harmonic potential function, the Chirikov-Taylor map [2], whose dynamics is two-dimensional. The dynamics of a periodically kicked rotor can be described in a periodic phase space $[-\pi, \pi) \times [-\pi, \pi)$, whose discrete-time variables p_n and x_n are, respectively, the momentum and the angular position of the rotor just after the n th kick, with the dynamics given by the following equations:

$$p_{n+1} = p_n + K \sin(x_n), \text{mod } 2\pi, \quad (3)$$

$$x_{n+1} = x_n + p_{n+1}, \text{mod } 2\pi, \quad (4)$$

where K is related to the kick strength.

In order to exemplify the dynamics of the Chirikov-Taylor map and its sticky phenomena, Fig. 1(a) displays a portion of the phase space for a typical trajectory of the system for $K = 3.0$. The denser areas near the island result from the sticky effect due to the time the trajectory remains near the edge of the island. To characterize the hyperbolicity of the surrounding areas of the island Fig. 1(b) displays the local angle between stable and unstable manifolds (θ), Eq. (2), near the resonant island. It is clear that the major part of the vicinities of the island is composed of strong nonhyperbolic areas, represented by dark blue (gray) areas in Fig. 1(b) (tangencies between UM and SM). A small fraction of the vicinity is observed

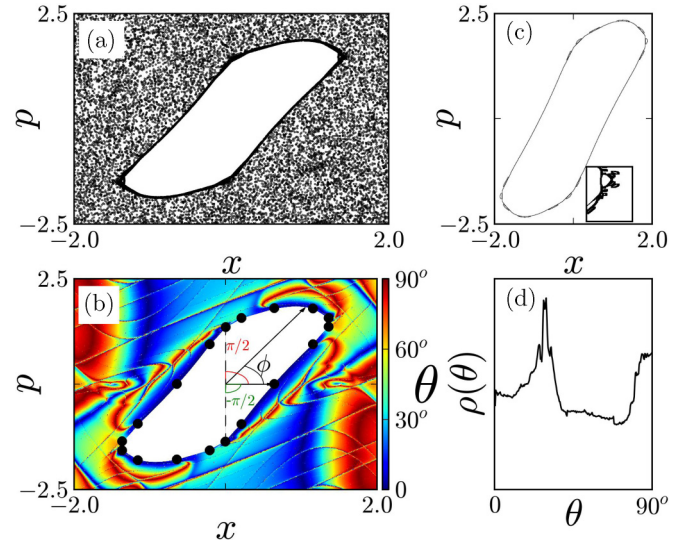


FIG. 1. (Color online) (a) Phase space for the kicked rotor map; darker regions around the main island reflect the effect of the stickiness. (b) Phase space distribution of angle between unstable and stable manifold; dark (blue) tones mean strong nonhyperbolicity. (c) An example of the edge detection algorithm used here to compute the vicinity of the island. In the inset we display magnification showing details of the edge. (d) Probability distribution function of the angle between stable and unstable manifolds, $\rho(\theta)$.

in red, yellow, and green (pale gray) tones and corresponds to angles greater than 30° and is responsible for the weak hyperbolic part of the vicinities. The role of both areas will be clear later in the text. In Fig. 1(b) we also define the angle $\phi = \arctan(p/x)$, defined in the interval $[-\pi/2, +\pi/2]$. Due to the symmetry of maps 3–4 we do not use the traditional $[-\pi, \pi)$ interval for ϕ since the hyperbolic properties and also locations of the fixed points of the left-hand side of the main island replicate those of the right-hand side. The 18 hyperbolic points located in the neighborhood of the main island are identified as black bullets in Fig. 1(b). The coordinates (x, p) and the angle ϕ of each one of the hyperbolic and elliptic points of period 18 in the neighborhood of the main island are shown in Table I. In order to make clear what we call the vicinity of the

TABLE I. Phase space position and polar angle of the 18 elliptic and hyperbolic points of period 18 in the neighborhood of the main island and the local maxima of $F_{\text{in}}^{100}(\phi)$.

Hyperbolic Points			Elliptic Points			max $[F_{\text{in}}^{100}(\phi)]$
x	p	ϕ	x	p	ϕ	
0.00	∓ 1.36	-1.57	± 0.09	∓ 1.20	-1.50	-1.57
± 0.21	∓ 0.95	-1.35	± 0.39	∓ 0.54	-0.95	-1.34
± 0.64	0.00	0.00	± 0.93	± 0.54	0.53	0.00
± 1.16	± 0.95	0.69	± 1.29	± 1.20	0.75	0.68
± 1.36	± 1.36	0.79	± 1.38	± 1.47	0.82	0.79
± 1.36	± 1.57	0.86	± 1.29	± 1.68	0.92	0.86
± 1.16	± 1.80	1.00	± 0.93	± 1.87	1.11	1.00
± 0.64	± 1.80	1.23	± 0.39	± 1.68	1.34	1.23
± 0.21	± 1.57	1.44	± 0.09	± 1.47	1.51	1.44

island, Fig. 1(c) displays the result of our algorithm for edge island detection [24], with details magnified in the inset. For numerical computation of the edge of an island, the algorithm considers a thick region surrounding all islands. The thickness parameter $\epsilon = 0.0025$ was used in all computed results.

Finally in Fig. 1(d) we plot the probability distribution function of the angles between SM and UM $\rho(\theta)$, so $\rho(\theta)d\theta$ represents the probability of finding an angle between θ and $\theta + d\theta$ in the phase space ensemble displayed in Fig. 1(b). The large plateau for small θ angles reflects the strong nonhyperbolic character of the region.

III. RESULTS

When a trajectory is initialized near the main island sticky area, but it is not a sticky trajectory, it leaves the vicinity of the island quickly following the unstable manifold of the hyperbolic points of period 18 located near the main island. To make it clear in Fig. 2(a) we plot the unstable manifold of the hyperbolic points of period 18 located near the main island, and Fig. 2(b) displays in red (gray) the phase portrait of many trajectories, initialized in a small circle in phase space and located near the vicinity of the main island. As can be

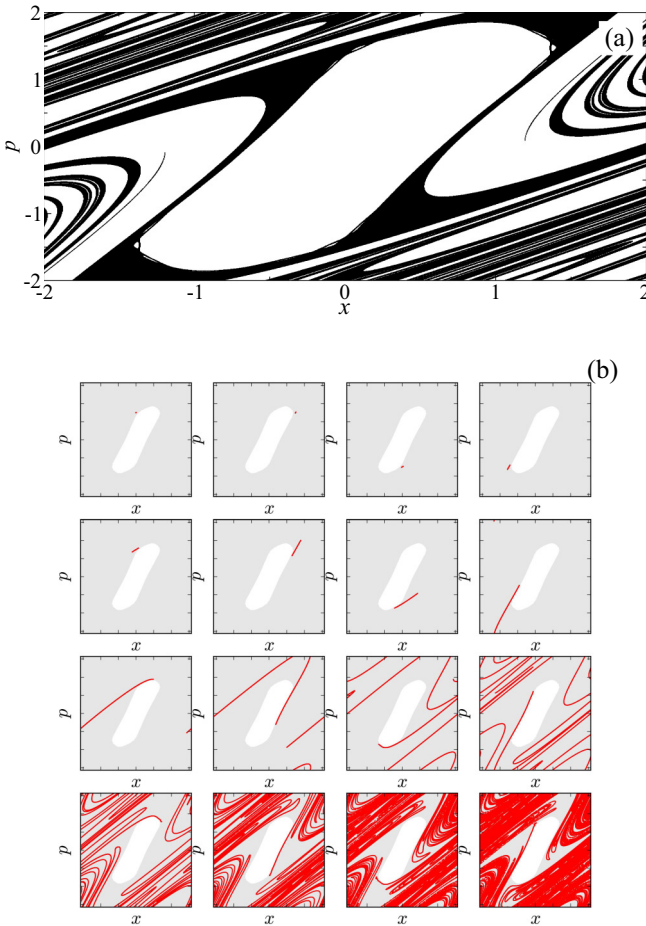


FIG. 2. (Color online) (a) Unstable manifold of the hyperbolic points of period 18 located near the main island. (b) Phase portrait of a bunch of trajectories initialized in a small region near the main island. As time goes on almost all trajectories leave the vicinity of the island following the unstable manifold.

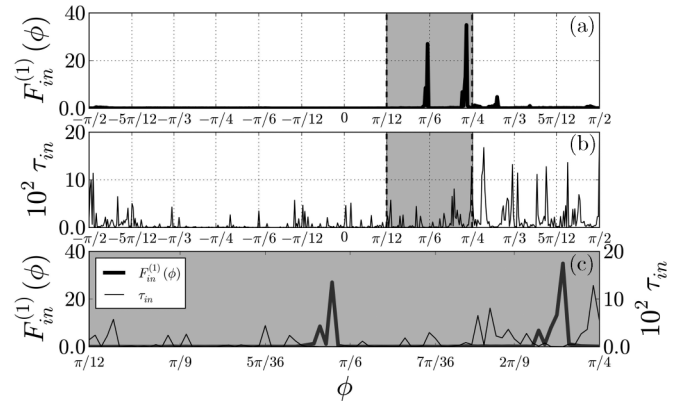


FIG. 3. (a) Probability distribution function of an income angle in the vicinity of an island on the Chirikov-Taylor map. (b) Average time spent in the sticky area as a function of the injected angle. (c) Magnification of panels (a) and (b) near the maxima of $F_{in}^{(1)}(\phi)$.

observed, almost all particles follow the unstable manifold displayed in black in Fig. 2(a). Just initial conditions started or injected almost tangent to the stable manifold remain near the island after just a few interactions.

The topological properties of the phase space in the vicinities of an island play an important role in the sticky mechanism. To explore the relation between topological characteristics of the phase space and the way trajectories visit an island vicinity and stick to it, we define the probability density function $F_{in}^{(1)}(\phi)$ for trajectories injected into the vicinity of the island considering the vicinity computed by our algorithm [Fig. 1(c)]. $F_{in}^{(1)}(\phi)d\phi$ is the probability that a typical chaotic trajectory will visit the vicinity of the island through an angle between ϕ and $\phi + d\phi$. In Fig. 3 we plot $F_{in}^{(1)}(\phi)$ [Fig. 3(a)] as well as the average time the trajectory remains in the vicinity of the island when injected in the vicinity by a particular angle [Fig. 3(b)]. In Fig. 3(c) we magnify the gray region of Figs. 3(a) and 3(b). Observe that although the major part of the trajectories are injected by just a few angles inside the red-yellow-green (light gray) tones of regions around the island in Fig. 1(a) (weak hyperbolic regions), these specific trajectories spend, on average, a short time mapping the sticky area. Trajectories are easily injected into the sticky areas by weak hyperbolic areas surrounding the island, but almost all of them are also easily ejected from it. Those trajectories do not contribute to the phenomena of stickiness and do not make any substantial changes in the Poincaré recurrence time for the dynamics.

In order to distinguish sticky trajectories from those that just reach the island edge and leave it quickly, we compute the probability density function $F_{in}^{(100)}(\phi)$ of trajectories injected into the sticky area by a specific angle considering that once a trajectory reaches the vicinity of the island, it remains mapping the same set of points as computed by our algorithm of island edges detection for at least 100 iterations. We identify such trajectories as sticky ones. Those trajectories are close related to the dynamics forced by the homoclinic tangle occurring near the main island [25,26]. In this scenario the occurrence of lobes in the phase space explains how a trajectory can stick in the boundary of an island, but the effectiveness of the sticky process is not theoretically fully understood. As a

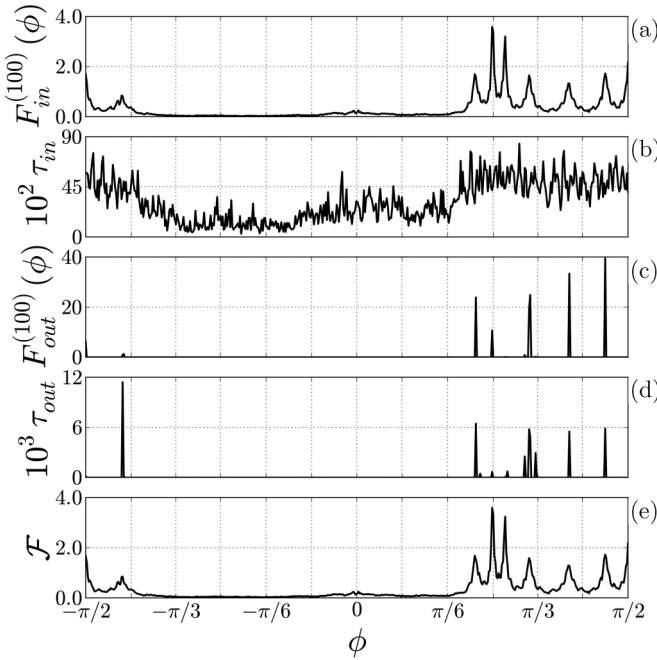


FIG. 4. (a) Probability distribution function of income angle into the right vicinity of the main island of the Chirikov map. The left side of the island displays symmetric results as pointed out in Table I. (b) Average spent time in the sticky area as a function of the injected angle. (c) Probability distribution function of the outcome angle from the vicinity of the main island of the Chirikov map. (d) Average spent time in the sticky area as a function of the ejected angle. (e) Probability distribution of the injected angle, subjected to the condition that the time of stickiness be greater than 1000 iterations.

result of the different levels of hyperbolicity of the regions around the main island, each hyperbolic fixed point region has its own characteristics allowing or prohibiting the injection and/or ejection of trajectories. For some hyperbolic points the lobes areas associated to it are very small. Additionally, in a scenario of strong nonhyperbolicity just lobes smashed near the hyperbolic fixed points contribute effectively to the injection and/or ejection of trajectories. Early evidence of this mechanism was reported in Ref. [27]. The dynamics resulting from this scenario is plotted in Fig. 4(a). Almost all sticky trajectories are injected in the vicinity of the island in very specific intervals of angles. Each angle interval is directly related to the angular location of the chain of periodic hyperbolic points [set as black bullets in Fig. 1(c)] and has its own maximum resulting from different levels of hyperbolicity of each region. This scenario leaves each hyperbolic fixed point vicinity to exhibit different rates of injection and/or ejection events. All trajectories that are not tangent enough to the stable manifold of the hyperbolic fixed point do not cross the tiny hyperbolic channel produced by the crossing between stable and unstable manifolds of the fixed point and cannot be injected into the stick area.

Considering those trajectories injected into the stickiness remaining mapping the edge for at least 100 iterations, we compute in Fig. 4(b) the average time they spend near the island (sticky trajectories) as a function of the injected angle. In Fig. 4(c) we graph the probability distribution function

of sticky trajectories as a function of the ejected angle $F_{out}^{100}(\phi)$. The almost discrete nature of the distribution is clear. All ejected trajectories follow the unstable manifold of the hyperbolic fixed points moving along a narrow channel departing from the fixed point. We plot in Fig. 4(d) the average time the trajectories stay in the sticky region (at least 100 iterations inside the sticky area) as a function of the outcome angle. From Fig. 4(d) we can conclude that sticky trajectories are ejected only by few angle intervals $\phi_{out} = \phi[\max(\tau_{out})]$. Therefore, we are able to calculate the probability $\mathcal{F}(\phi)d\phi$ that a given trajectory will enter the sticky region considering only trajectories that leave these region through the angle ϕ_{out} . The result is plotted in Fig. 4(e). The great similarity between \mathcal{F} and $F_{in}^{(100)}$ suggests that our previous conclusions are consistent. Therefore, we can argue that the local maximum of $F_{in}^{(100)}$ represents the sticky angles, i.e., the angles that, once a trajectory is injected from one of them, there is a great probability that this trajectory turns out to be stuck to the island. These maxima correspond to the same region where hyperbolic points are located, confirming the hypothesis that these points provide a channel for a typical trajectory to enter in the sticky region. Figures 4(a) and 4(e) clearly show that both figures are almost identical, a strong suggestion that all trajectories leave the sticky regions by the hyperbolic channels departing from the hyperbolic fixed points.

The presence of stickiness around an island is predicted by theory [4,18], but an analysis of Fig. 4(a) shows that the effectiveness of a trajectory injection or ejection by a particular hyperbolic channel is not the same for all fixed points, as can be observed by the different amplitudes of maxima of $F_{in}^{(100)}$ in Fig. 4(a). In order to make clear the role of the hyperbolicity of the close vicinity of the hyperbolic fixed points in the injection and ejection phenomena of sticky trajectories, first, we present as an example in Fig. 5(a) the degree of hyperbolicity of one of the hyperbolic points of period 18 located around the main island of the Chirikov-Taylor map. As observed in Fig. 5(b) the probability density function $\rho(\theta)$ exhibits just a sharp maximum due to the almost unique angle between a stable and unstable manifold computed in the close vicinity of the fixed point. All other fixed points display similar sharp peaks in the probability density function $\rho(\theta)$; nevertheless each hyperbolic point has its own angle for the maximum of $\rho(\theta)$ characterizing its own *degree of hyperbolicity*. Second, to demonstrate the relation between the degree of hyperbolicity of

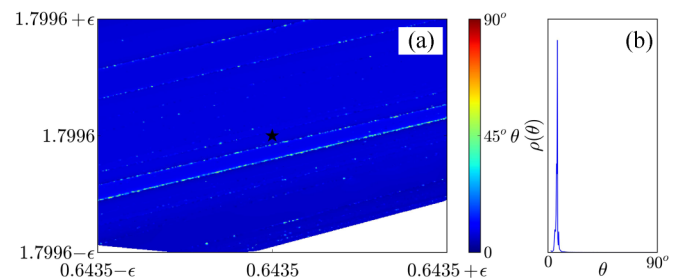


FIG. 5. (Color online) (a) Degree of hyperbolicity of the vicinity ($\epsilon = 0.0025$) of one of the 18 fixed points located around the main island of map 4. (b) $\rho(\theta)$ characterized by just one maximum when computed near a fixed point around the main island.

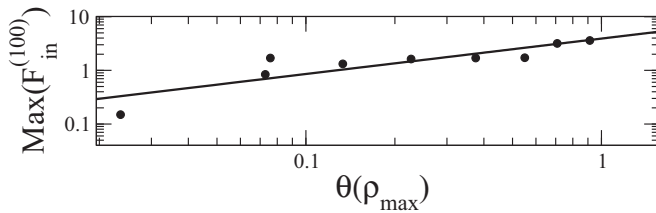


FIG. 6. The effectiveness of the injection channels measured using $\max F_{\text{in}}^{(100)}$ as a function of the angle between UM and SM.

the close vicinity of the fixed points, and the effectiveness of the hyperbolic channels related to each fixed point to capture sticky trajectories, we graph in Fig. 6 the maxima of the function $F_{\text{in}}^{(100)}(\phi)$ as a function of the degree of hyperbolicity measured by the angle for which the function $\rho(\theta)$ exhibits a maximum $\theta(\rho_{\text{max}})$. The black line is a power law fitting that serves us as a guide to the eye. The result displayed in Fig. 6 clearly shows that the effectiveness of the channels is a function of the degree of hyperbolicity of the close region of the fixed points. Small values of $\theta(\rho_{\text{max}})$ are related to the fact that just a very small portion of the surrounding area of the fixed point is occupied by the injection and/or ejection hyperbolic channel. As a result the function $F_{\text{in}}^{(100)}(\phi)$ reveals a relatively small maximum, meaning that just a small fraction of trajectories can cross the channel in an injection or ejection process from the sticky area.

Such properties of the phase space allow us to manipulate the nonequilibrium fluctuation of the system. To show that it is possible to control the nonequilibrium fluctuations that arise due to the presence of stickiness, we track the position of the trajectory, and once it maps small circles of radius 0.003 (corresponding to $\approx 1 \times 10^{-5}\%$ of the phase space) centered in each of the hyperbolic points of period 18, we perturb the trajectory, so a possible crossing of the channel and consequent stick of the trajectory is avoided. Numerically, we perform a restart of the trajectory outside the injection channel. Results for the Poincaré recurrence time for the system with and without the control mechanism for two values of K , $K = 3.0$ and $K = 3.565$ (a large stickiness case), are plotted in Fig. 7. Black bullets and a green up-triangle display the time distributions for Poincaré recurrence without any control mechanism. As can be observed for large recurrence time, a strong fluctuation of the exponential law is observed. In fact for large recurrence time the distribution has a power law decay as a result of the sticky phenomena in the recurrence time. The time distribution of the Poincaré recurrence time for the system subjected to our control mechanism is displayed as red squares and a blue down-triangle. For this case, almost all fluctuation for long recurrence time is absent, corroborating the idea that

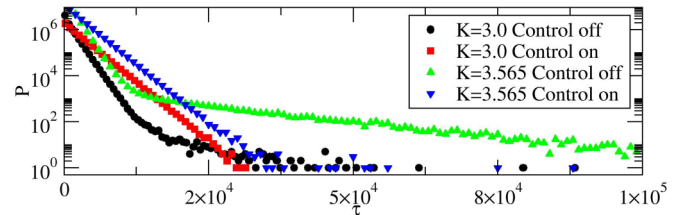


FIG. 7. (Color online) Recurrence time for the Chirikov-Taylor map with and without control.

all nonequilibrium fluctuation in the system is now absent since the stickiness is avoided. Additionally we observe that the exponential rate for both K values is the same, supporting the idea that the behavior of the system is now completely diffusive independently of the K value. All results here are presented for two values of K , but similar results are obtained for other values of the nonlinear parameter.

IV. CONCLUSIONS

We have described in this paper a mechanism to suppress the effect of stickiness based on the knowledge of the nonhyperbolic structures on the edge of an island of a Hamiltonian two degrees-of-freedom system. We have shown that the effectiveness of an island edge to sticky trajectories is directly related to the degree of hyperbolicity of small areas surrounding hyperbolic points around the island. The vicinity of the island is composed of two very distinct characteristics, namely, a strong nonhyperbolic region and, superposed on it, hyperbolic tinny channels related to stable manifolds of hyperbolic points located in the vicinity. We have shown that monitoring those vicinity areas of the phase space, it is possible to generate a normal diffusive processes without (almost) any influence of the large recurrence time due to the stickiness phenomena. Our control mechanism turns the original power law fitted recurrence time distribution for the system into a exponential fitted time distribution, avoiding the system from exhibiting extreme events in the dynamics. Moreover, once under control, we can turn the original nondiffusive system into a diffusive one, applying control of small portions of phase space.

ACKNOWLEDGMENTS

This work has had partial financial support from CNPq (Grants No. 302950/2013-3 and No. 552148/2011-3) (PROCAD), CAPES, and Fundação Araucária (Brazil). Computer simulations were performed at the LCPAD cluster at Universidade Federal do Paraná, supported by FINEP (CT-INFRA).

- [1] G. M. Zaslavsky, *Hamiltonian Chaos and Fractional Dynamics* (Oxford University Press, New York, 2005).
- [2] A. J. Lichtenberg and M. A. Leiberman, *Regular and Chaotic Dynamics* (Springer, Berlin, 1992).
- [3] G. M. Zaslavsky, *Phys. Rep.* **371**, 461 (2002).

- [4] J. D. Meiss and E. Ott, *Phys. Rev. Lett.* **55**, 2741 (1985).
- [5] R. Venegeroles, *Phys. Rev. Lett.* **101**, 054102 (2008); **102**, 064101 (2009).
- [6] E. G. Altmann and T. Tel, *Phys. Rev. Lett.* **100**, 174101 (2008).

- [7] J. M. Seoane and M. A. F. Sanjuán, *Phys. Lett. A* **372**, 110 (2008).
- [8] E. G. Altmann and A. Endler, *Phys. Rev. Lett.* **105**, 244102 (2010).
- [9] Y.-C. Lai and T. Tél, *Transient Chaos Complex Dynamics on Finite-Time Scales* (Springer, New York, 2010).
- [10] O. Alus, S. Fishman, J. D. Meiss, [arXiv:1410.7648v1](https://arxiv.org/abs/1410.7648v1) [nlin.CD].
- [11] R. W. Easton, J. D. Meiss, and S. Carver, *Chaos* **3**, 153 (1993).
- [12] S. R. Lopes, J. D. Szezech Jr., R. F. Pereira, A. A. Bertolazzo, and R. L. Viana, *Phys. Rev. E* **86**, 016216 (2012).
- [13] A. Babiano, G. Boffetta, A. Provenzale, and A. Vulpiani, *Phys. Fluids* **6**, 2465 (1994).
- [14] T. Tél, A. de Moura, C. Grebogi, and G. Károlyi, *Phys. Rep.* **413**, 91 (2005).
- [15] J. D. Szezech Jr., I. L. Caldas, S. R. Lopes, P. J. Morrison, and R. L. Viana, *Phys. Rev. E* **86**, 036206 (2012).
- [16] C. Efthymiopoulos, G. Contopoulos, and N. Voglis, *Celestial Mech. Dyn. Astron.* **73**, 221 (1999); M. Harsoula, C. Kalapotharakos, and G. Contopoulos, *Mon. Not. R. Astron. Soc.* **411**, 1111 (2011).
- [17] G. M. Zaslavsky, *Physica D* **168-169**, 292 (2002).
- [18] L. A. Bunimovich and L. V. Vela-Arevalo, *Chaos* **22**, 026103 (2012).
- [19] R. S. Mackay, J. D. Meiss, and I. C. Percival, *Physica D* **13**, 55 (1984).
- [20] J. Guckenheimer and P. Holmes, *Nonlinear Oscillations, Dynamical Systems, and Bifurcations of Vector Fields* (Springer, New York, 2002).
- [21] C. Grebogi, S. M. Hammel, J. A. Yorke, and T. Sauer, *Phys. Rev. Lett.* **65**, 1527 (1990).
- [22] Y. C. Lai, C. Grebogi, J. Yorke, and I. Kan, *Nonlinearity* **6**, 779 (1993).
- [23] F. Ginelli, P. Poggi, A. Turchi, H. Chaté, R. Livi, and A. Politi, *Phys. Rev. Lett.* **99**, 130601 (2007).
- [24] S. Benkadda, S. Kassibrakis, R. B. White, and G. M. Zaslavsky, *Phys. Rev. E* **55**, 4909 (1997).
- [25] S. Wiggins, *Global Dynamics, Phase Space Transport, Orbits Homoclinic to Resonances, and Applications* (American Mathematical Society, Providence, RI, 1993).
- [26] V. Rom-Kedar and S. Wiggins, *Arch. Ration. Mech. Anal.* **109**, 239 (1990).
- [27] I. Dana and S. Fishman, *Physica D* **17**, 63 (1985).